LARGE-SCALE LABORATORY TRIALS OF SELF-HEALING TECHNOLOGIES

Sripriya Rengaraju*, *Christos* Vlachakis, *Vahid* Afroughsabet, and *Abir* Al-Tabbaa

Department of Engineering, University of Cambridge, Cambridge, UK

Abstract. Prolonging the life of the reinforced concrete structure is the most promising solution to reduce the carbon emissions from concrete. To achieve that, the structure should be protected from crack formation, which acts as an easy pathway for deleterious agents. Self-healing technologies are intended to provide long-term resilience against cracking due to various deterioration processes. Technologies that performed well in small, laboratory-scale studies are taken to the next level to assess their performance on a larger scale and monitored using various NDT equipment. A 1m long beam with a cross-section (140×120 mm) was cast with two rebars – one with a cover depth of 50 mm from the top and another with a cover depth of 20 mm from the bottom. The mix design consists of CEM IIIA (50 OPC: 50 Slag) cement and 30% lightweight aggregate as a replacement for coarse aggregate. At 28 days of curing, the concrete beams are subjected to accelerated corrosion (by applying a voltage to the bottom rebar) to induce internal cracking. Once internal cracking is induced, the beams are subjected to another 28 days under water for healing. The performance of the beams is monitored via ultrasonic pulse velocity and half-cell potential before and after voltage application. This paper shows the preliminary results and the self-healing efficiency and corrosion resistance of these beams are continuously being monitored under severe chloride conditions to predict the long-term performance.

1 Introduction

Crack formation arising due to a variety of loading conditions (mechanical and environmental) is identified as the main issue and starting point of deterioration as it allows the ingress of moisture and deleterious agents through concrete. Self-healing systems are promising solutions addressing the crack formation without manual interventions - ideally, improving the durability without a significant increase in maintenance cost. A variety of self-healing additives in the form of microcapsules, smart aggregates, super absorbent polymers, and fibres are being used to mitigate the adverse effects of crack formation and heal the cracks in concrete without any human intervention.

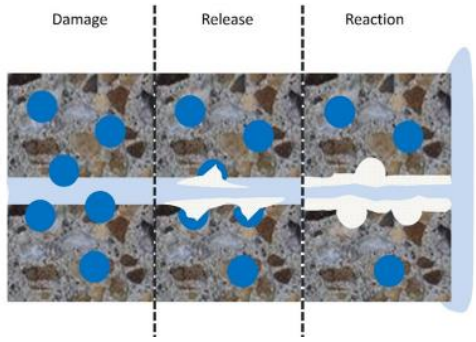

Fig. 1. Self healing mechanism in concrete with additives [1]

The self-healing agents made available at the crack location by the additives, start the healing process either by exposure to air or by reacting with the cementitious matrix as shown in Figure 1. Hence, it is essential to disperse the additives uniformly to optimise the performance of self-healing. It is reported that there is a discrepancy in the performance of self-healing additives when comparing small scale laboratory specimens to large scale field applications, attributing it to size effect [2]. In addition, there are very few case studies related to large scale applications of self-healing additives in concrete. In the UK, microcapsules have been used in a retaining wall and a slab [3,4]. Similarly, macrocapsules, glass tubes with self-healing agents have been used in large scale reinforced beams [5,6]. However, there are not enough evidence/trials with self-healing concrete performing better or as expected in these large-scale applications in field trials. Hence, it is necessary to establish the efficiency of the self-healing concrete in large scale specimens under severe or realistic conditions.

Usually, laboratory tests are done in mortar or concrete in small scale specimens immediately after 28 days of curing and mechanical tests are performed to induce the crack formation and self-healing performance is monitored. The self-healing efficiency is assessed in terms of mechanical strength recovery, water ingress, and crack healing after a certain period of time where the concrete was allowed to come in contact with water. This condition is ideal for the performance as

* Corresponding author: sr973@cam.ac.uk

water is always available and the concrete has a lot of portlandite which can help in the healing process. However, the main idea of self-healing concrete is the availability of healing process after a certain period of exposure to real life conditions. If the cracking occurs due to internal deterioration or ageing, the performance of the self-healing additives is mostly unknown [7]. Currently, there is no standard accelerated test method or ageing test which can simulate the exposure conditions and establish the long-term performance [8]. This is a major limitation in implementing the self-healing additives in the field as their performance in aged structures where it was supposed to work is unknown. In addition, the non-destructive testing (NDT) methods, which have the standard values established for traditional concrete systems are out of range or not applicable to the self-healing systems. One can make a comparative assessment of self-healing systems but not comply with the standards [9]. In such cases, there is a chance of misinterpretation of data due to a lack of experience with such concretes and need further investigation to establish the range of test values. Another gap in this self-healing concrete research is the lack of studies related to self-healing efficiency in low carbon binders with self-healing additives. Even though the self-healing efficiency of the additives such as bacterial spores, SAP, and fibres are well established in low carbon cements, the self-healing efficiency of the additives which primarily react with portlandite to produce the self-healing products is largely unknown [10].

This paper deals with self-healing additives in low carbon binders in large scale specimens. In addition, it also presents the self-healing efficiency of the specimens when subjected to internal corrosion to induce the crack formation.

2 Methodology

Concrete beams with dimensions of 120×140×1000 mm and different self-healing technologies were prepared and their performance after exposure to harsh environment was monitored. Table 1 shows the mix design of concrete followed in this experiment.

Table 1. Mix design for 1m^3 of concrete

Ingredients	Quantity (kg)
CEM III (50% Cement:50%Slag)	360
Water	180
Fine aggregate	790.6
Coarse aggregate	522.35
Lightweight aggregate (Lytag: 4-14 mm)	223.87

CEM III cement was used as nowadays CEM I is no longer encouraged. The water to cement ratio was kept at 0.5. Sharp sand and gravel with a maximum size of 2 mm and 11.2 mm were utilized in this mix design. In addition, 30% of coarse aggregate was replaced by light weight aggregates. The lightweight aggregates were procured from Lytag® lightweight solutions. Lytag aggregates are fly ash based aggregates formed using a sintering process. This concrete was taken as the base design for control mix and the self-healing additives were added to this mix for self-healing concretes. Sikament 700 superplasticiser supplied by Sika Ltd, Hertfordshire, UK was used in concrete mixes as a water reducing admixture to adjust the workability of concrete mixes (if needed).

For reinforcement, two rebars of 8 mm size were placed in the beam; one at 50 mm from the top surface of the concrete and 20 mm from the bottom surface respectively as shown in Figure 2. The beams were designed such that assessment of accelerated corrosion and the cracking will be done in the lower rebar. The other rebar was placed in the middle to assess the effect of macrocell corrosion and further quantification of effect of self-healing systems on the transport properties. Three sets of specimens were cast, namely the control mix without any additives, and two self-healing concrete mixes where the optimum doses of self-healing additives were added. Superabsorbent polymer (SAP) produced by BASF and polypropylene fibers produced by Sika was added as self-healing concrete mixes at the dosage of 0.5% by the weight of binder respectively and are shown in Figure 3.

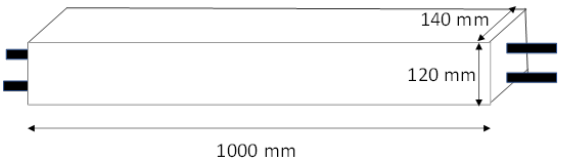

(a) Beam dimensions

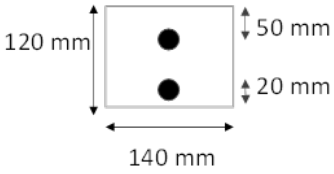

(b) Cross section

Fig. 2. Dimensions of large scale beam specimens

The mixing procedure was done as follows: the binder and fine aggregate were mixed initially for 1 min, and half of the mixing water was added and mixed for 2 min. In the case of SAP admixed concretes, the SAP was also added to the dry binder and fine aggregate. The coarse aggregate was then added along with the remaining water, and superplasticizer and mixed for 3 min. For fiber-reinforced specimens, fibers were added to the mix as the last ingredient and mixing was continued for an additional 5 min. Water absorption and moisture content correction were considered for the aggregates. To avoid any adverse effect on the workability of concrete mixes, lightweight aggregates (Lytag) were soaked in water for 24 hours and then sieved and used in saturated surface dry (SSD) condition.

(a) PP fibres (b) SAP (c) Lytag

Fig. 3. Materials used in the concrete mix design

Two specimens were cast for each mix design and a total of six beams were cast. All the large-scale specimens were cured for 28 days in a water bath containing lime to avoid leaching. Three 100×100×100 mm cube specimens were also cast along with the large-scale beams to determine the compressive strength.

At 28 days of curing, an impressed voltage of 60V was applied for 6 hours on the bottom rebar to induce microcracking in concrete beams because of accelerated corrosion. A minimum amount of salt (0.035% of NaCl) was added to the solution to increase the conductivity of the electrolyte and accelerate the corrosion process. A stainless-steel mesh was used as a cathode and was kept parallel to the beam in solution. The level of the solution was kept at the level of the bottom rebar to ensure that the induced voltage does not affect the top rebar. This voltage was chosen for two reasons, namely (i) the specimen was larger, and it needed higher voltage to induce the microcracking and (ii) to reduce the time of voltage application required to induce the cracking. The concrete cover of 20 mm is chosen to monitor the self-healing performance of samples for internal cracking. Figure 4 shows the test setup for the accelerated corrosion process. The specimen was also embedded with a variety of sensors to monitor its performance. However, those details are not included in this paper.

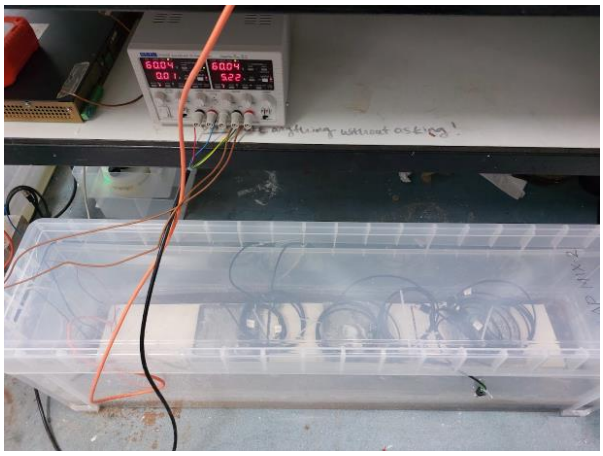

Fig. 4. Test setup for accelerated corrosion

Two types of NDT tests are discussed in this paper. The first one is ultrasonic pulse velocity (UPV) and the second one was half-cell potential. These two tests were performed at 28 days of curing before and after the application of voltage. 10 points at a distance of 10 cm centre to centre were marked on the sides of the beam. The first and last point was at a distance of 5 cm from the edges of the beam. These 10 points were marked at the same level as that of the lower rebar, which was also impressed with voltage. Similarly, these 10 points were marked at the bottom of the beam. The UPV was done in two ways, namely direct transmission measuring the pulse velocity when the probes were kept at opposite sides of the beam and indirect transmission by keeping one of the probe on one side of the beam and the other probe on the bottom surface of the beam. This kind of testing was done to capture any microcrack induced along the sides or bottom of the beam due to internal corrosion of the embedded steel. Similarly for capturing the corrosion potential, the potential difference was measured using a multimeter by connecting the reference electrode, which was kept at each of the 10 points on one side of the beam on the concrete surface and the rebar. The surface was made wet to ensure proper ionic conductivity was established.

3 Results and Discussion

The compressive strength results are discussed first followed by the tests on UPV. In UPV, both the direct and indirect transmission results are presented.

3.1 Compressive strength

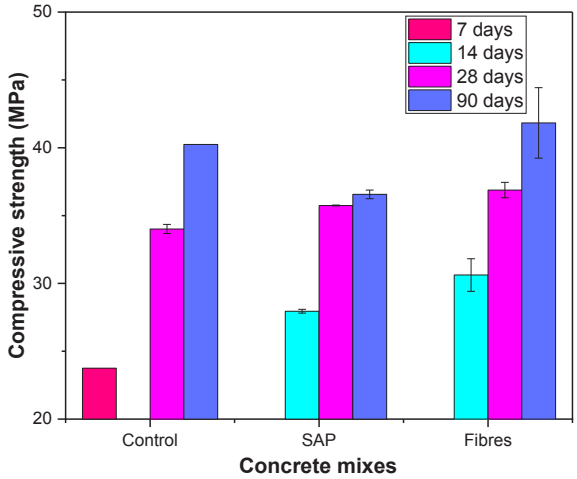

Fig. 5. Compressive strength of concrete at different ages of curing

Figure 5 shows the compressive strength evolution of concrete mixes at different ages of curing. The concrete mix with SAP additives has slightly lower compressive strength compared to the other mixes. This may be due to absorption of water by the SAP in fresh state, which could have led to less water available for hydration The cube specimens were kept at 100% relative humidity by placing them above the saturated sand in a tub and were not immersed in water. Hence, there was no extra water available from the curing process for the SAP specimens. In the case of fibre reinforced mixes, there was no adverse effect. This agrees with the literature. It is to be noted that there is an increase of 10 MPa as the concrete ages. The slag in the concrete which acts as a latent binder reacts with portlandite and calcium within itself and produces secondary C-S-H. This reaction causes the increase in strength at later ages. Therefore, there is an increase in strength at 90 days, which is also in agreement with the literature [11].

3.2 Ultrasonic pulse velocity (UPV)

The UPV test was done with the help of Proceq UPV equipment which had a short-range probe to measure the pulse velocity (m/s). Figure 6 shows the readings of the pulse velocity measured via direct and indirect transmission methods in control specimens. The values measured via indirect transmission were higher than the values measured via direct transmission as the distance travelled is not the shortest route and is as expected. In general, there is a decrease in pulse velocity from the baseline once the voltage is applied. This is agreeable and is expected as the accelerated corrosion might have induced microcracking [9].

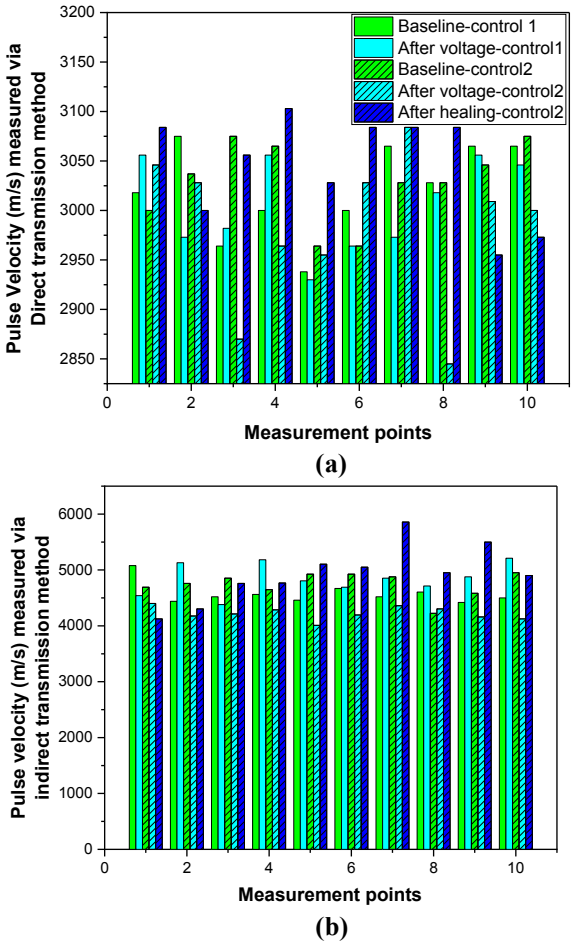

Fig. 6. Pulse velocity measurements in control specimens (a) direct transmission method (b) indirect transmission method

There are some discrepancies such as increase in pulse velocity in some of the points (points 1,3, and 4 in Control 1; points 6 and 7 in Control 2). This could be due to the mild corrosion (0-4%) in those points which enhances the bond [12] and hence the pulse velocity.In such points, the corrosion is not enough to induce cracking; however, the corrosion products might have created a dense film in the interface region causing an increase in the pulse velocity. In some of the specimens, there were outliers, which could be due to handling issues during testing and can be safely excluded from concluding remarks as they were very small in number. Another thing to note here is the UPV reading after 28 days of healing under water. There is an increase in values measured after healing. However, it was very difficult to interpret whether the increase was due to healing or hydration evolution because of slag. Moreover, the time frame needed for carrying out these tests and handling of specimens were imposing certain limitations and hence, the healing data could not be obtained for other specimens and are being collected now.

Figure 7 and Figure 8 show the pulse velocity measured in SAP and fibre specimens respectively. In Sap specimens, there are some outlier readings such as point 7 and point 9 in Figure 6 (a) and (b) respectively. As mentioned earlier, such outliers can be neglected without losing much data for interpretation. Similarly, points 9 and 10 had outliers in fibre reinforced specimens and were not considered for analysis. In general, a similar trend in the UPV measurements i.e., decrease in the value after induced corrosion was observed. Even though the mechanisms of the additives are different, they followed the same trend and the UPV was able to capture the reinforcement corrosion and associated microcracking in these specimens. Hence, it can be concluded that UPV values from the specimens with reinforcement were also good indicators of understanding the deterioration and were able to indicate the possibility of ongoing corrosion.

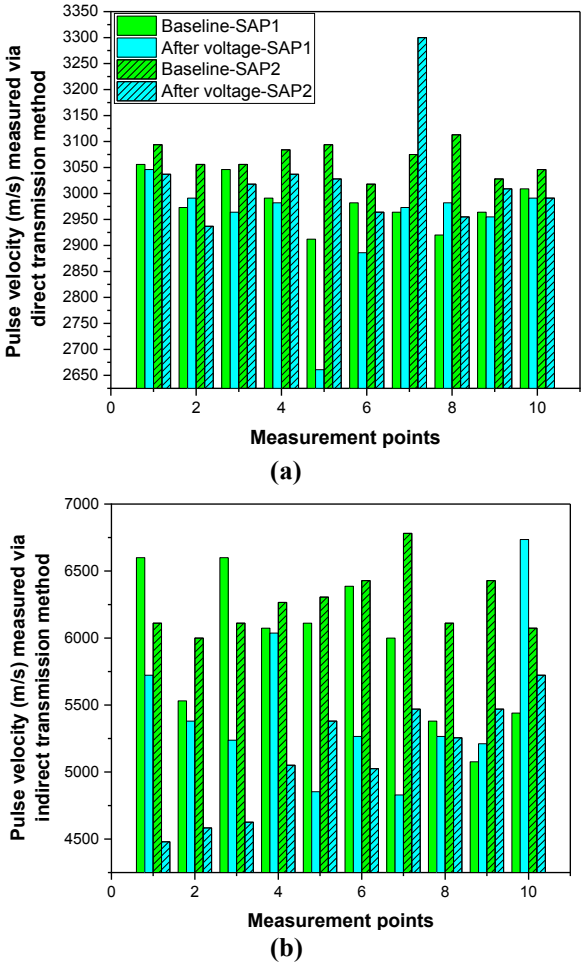

Fig. 7. Pulse velocity measurements in SAP specimens (a) direct transmission method (b) indirect transmission method

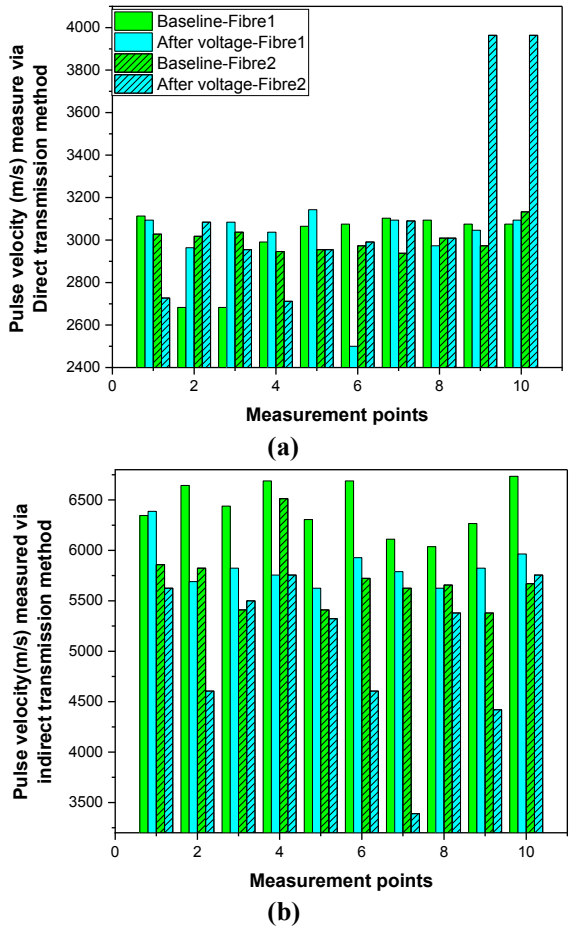

Fig. 8. Pulse velocity measurements in fibre specimens (a) direct transmission method (b) indirect transmission method

3.3 Half-cell potential

Figure 9 shows the half-cell potential measured using Ag/AgCl reference electrode. Here, only the results from specimen 2 of each mix are shown.

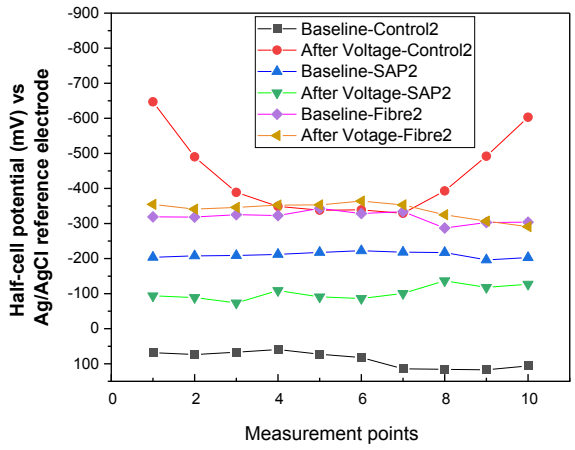

Fig. 9. Half-cell potential measured in the beams before and after voltage application

There is a significant decrease in potential in the control specimen after voltage application. The half-cell potential at the ends were significantly lower as the voltage connection was at the ends and the specimens were corroded more at the ends compared to the middle of the beam in the control specimen. However, the SAP specimen had an increase in potential after voltage application. This behaviour was slightly strange as it is expected that the potential should decrease. Additionally, it does not comply with the UPV results as the UPV results decrease after voltage application and hence require further investigation. On the other hand, the values from the fibre specimen were similar to the control specimen showing a decreasing trend in potential values. So, it is essential to investigate the half-cell potential in these novel self-healing concrètes to further understand its effect on cracking and corrosion to make the data interpretation becomes more reliable.

4 Conclusions

The long-term tests are ongoing and the following preliminary conclusions were made from the NDT tests done after 28 days of curing

1) The compressive strength was not affected significantly by the addition of SAPs or fibres. A proper mix design will help to get the desired strength.
2) UPV measurements indicated the ongoing corrosion - a decrease in the values was observed with corrosion. This trend was observed irrespective of the mix design.
3) The half-cell potential on the bottom rebar indicated the corrosion initiation in control and fibre specimens. However, the SAP did not follow the trend and requires further investigation.

The authors would like to acknowledge Dr Yen-Fang Su and Dr Livia Ribeiro de Souza for their assistance during casting.

References

[1] C. Litina, A. Al-Tabbaa, First generation microcapsule-based self-healing cementitious construction repair materials, Constr. Build. Mater. 255 (2020) 119389. https://doi.org/10.1016/j.conbuildmat.2020.11938.

[2] R. Alghamri, S. Rengaraju, A. Al-Tabbaa, Large-scale laboratory trials of smart aggregates for self-healing in concrete under different curing regimes, Cem. Concr. Compos. 136 (2023) 1–31. https://doi.org/10.1016/j.cemconcomp.2022.10484

[3] C. Litina, B. Cao, J. Chen, Z. Li, I. Papanikolaou, A. Al-Tabbaa, First UK Commercial Deployment of Microcapsule-Based Self-Healing Reinforced Concrete, J. Mater. Civ. Eng. 33 (2021) 1–15. https://doi.org/10.1061/(asce)mt.1943-5533.0003702.

[4] A. Al-Tabbaa, C. Litina, P. Giannaros, A. Kanellopoulos, L. Souza, First UK field application and performance of microcapsule-based self-healing concrete, Constr. Build. Mater. 208 (2019) 669–685. https://doi.org/10.1016/j.conbuildmat.2019.02.178.

[5] K. Van Tittelboom, J. Wang, M. Araújo, D. Snoeck, E. Gruyaert, B. Debbaut, H. Derluyn, V. Cnudde, E. Tsangouri, D. Van Hemelrijck, N. De Belie, Comparison of different approaches for self-healing concrete in a large-scale lab test, Constr. Build. Mater. 107 (2016) 125–137. https://doi.org/10.1016/j.conbuildmat.2015.12.18

[6] E. Tsangouri, J. Lelon, P. Minnebo, H. Asaue, T. Shiotani, K. Van Tittelboom, N. De Belie, D.G. Aggelis, D. Van Hemelrijck, Feasibility study on real-scale, self-healing concrete slab by developing a smart capsules network and assessed by a plethora of advanced monitoring techniques, Constr. Build. Mater. 228 (2019) 116780. https://doi.org/10.1016/j.conbuildmat.2019.11678

[7] N. De Belie, E. Gruyaert, A. Al-Tabbaa, P. Antonaci, C. Baera, D. Bajare, A. Darquennes, R. Davies, L. Ferrara, T. Jefferson, C. Litina, B. Miljevic, A. Otlewska, J. Ranogajec, M. Roig-Flores, K. Paine, P. Lukowski, P. Serna, J.M. Tulliani, S. Vucetic, J. Wang, H.M. Jonkers, A Review of Self-Healing Concrete for Damage Management of Structures, Adv. Mater. Interfaces. 5 (2018) 1–28. https://doi.org/10.1002/admi.201800074.

[8] T. Van Mullem, G. Anglani, M. Dudek, H. Vanoutrive, G. Bumanis, C. Litina, A. Kwiecień, A. Al-Tabbaa, D. Bajare, T. Stryszewska, R. Caspeele, K. Van Tittelboom, T. Jean-Marc, E. Gruyaert, P. Antonaci, N. De Belie, Addressing the need for standardization of test methods for self-healing concrete: an inter-laboratory study on concrete with macrocapsules, Sci. Technol. Adv. Mater. 21 (2020) 661–682. https://doi.org/10.1080/14686996.2020.1814117

[9] X. Huang, S. Kaewunruen, Self-healing concrete, INC, 2020. https://doi.org/10.1016/B978-0-12-818961-0.00027-2.

[10] K. Van Tittelboom, N. De Belie, Self-healing in cementitious materials-a review, 2013. https://doi.org/10.3390/ma6062182.

[11] I. Barišić, S. Dimter, T. Rukavina, Strength properties of steel slag stabilized mixes, Compos. Part B Eng. 58 (2014) 386–[7391. https://doi.org/10.1016/j.compositesb.2013.11.002.

[12] A.A. Almusallam, A.S. Al-Gahtani, A.R. Aziz, Rasheeduzzafar, Effect of reinforcement corrosion on bond strength, Constr. Build. Mater. 10 (1996) 123–129. https://doi.org/10.1016/0950-0618(95)00077-1.